Segmentation of Compound Signals Using Higher-Order Activity Indexes

Damjan Zazula and Rok Istenič

***Abstract*—**The so called activity index is defined on the second-order statistics. In multiple-input multiple-output (MIMO) models, it estimates the level of activity of individual input sources. In this paper, we study an extended definition of activity index, which deploys higher-order statistics instead of the second-order. Experiments with synthetic models show that noise resistance at higher even orders increases. In spite of the fact that the level of superimpositions of source activity also increases, which is disturbing, a difference of the 4^{th}- and 2^{nd}-order activity indexes proves to be a reliable relative measure of the number of simultaneously active input sources. The measure is not influenced either by the properties of sources, or by the level of additive random Gaussian noise, or the over- or underdeterminancy of the model output observations. This can be of considerable help when analysing and, in particular, decomposing compound MIMO output signals.

***Keywords*—**Activity index, Compound signal segmentation, Higher-order moments, MIMO models, Sparse signal sources.

I. Introduction

System identification or signal and image detection in many fields of applications are faced with compound observations. Telecommunications, seismic and radar measurements, speech processing, medical diagnosing are some typical cases. To extract useful information based on these observations, efficient analysis methods have been developed to estimate the measured signals, transmission channels, and signal sources. Recently, research was intensified in the field of blind analysis techniques that try to identify properties of system channels and signal sources when only received or observed signals are available [6]. These cases can be modelled in multiple-input multiple-output sense (MIMO). When the model inputs can be considered orthogonal, many blind source separation (BSS) techniques are available to separate the sources. Robust and successful solutions have been reported for telecommunications [1], seismic and radar signals [2], speech processing [3], bioelectrical signals [4], and image processing [5].

Manuscript received August 21, 2010. This work was supported in part by the Slovenian Research Agency, Grant P2-0041 "Computer Systems, Methodologies, and Intelligent Services."

Damjan Zazula is with University of Maribor, Faculty of EE and CS, Smetanova 17, 2000 Maribor, Slovenia (corresponding author–phone: +386 2 220 74 80; fax: +386 2 220 72 72; e-mail: zazula@uni-mb.si).

Rok Istenič is with University of Maribor, Faculty of EE and CS, Smetanova 17, 2000 Maribor, Slovenia (e-mail: rok.istenic@uni-mb.si).

Even if source signals are only close-to-orthogonal and if the number of observations does not guarantee overdeterminancy, some algorithms can cope with their separation. A very successful one was proposed in [8]. Although it was basically built for the cases where sources produce only a limited number of finite symbols (source activity), it means a novel and general paradigm in the field of compound signal decomposition. When finite symbols are sent through a transmission channel, they are convolved by the channel responses and contribute to the system output as observations of transmitted symbols. Bioelectrical signals, such as electrocardiograms (ECG), can be modelled with entirely orthogonal sources (no overlap is possible between different types of heart beats, e.g. normal systoles and extrasystoles), while electromyograms (EMG) lose orthogonality by increasing muscle contraction forces [11], [15]. The number of overlapping motor-unit action potentials (MUAP) increase with higher contraction forces [9]. On the other hand, when observing certain types of communications, such as CDMA [1], orthogonality of sources may be supposed as well.

Compound signal decomposition aims at the detailed information on the properties of individual separated signal sources. Different applications, such as medical diagnosing or communication channel multiplexing, highly benefit from it. However, more global indications are also important, such as the number of sources, duration of their responses, or the amount of their overlapping [9]. These may help improve the signal decomposition results or just assess the observed measurements quickly, possibly in real time.

Some time ago, we developed a blind signal decomposition method called Convolution Kernel Compensation (CKC) [8], [10]. The method has proved itself with a high rate of properly decomposed surface elecromyograms. The initial decomposition step is based on a global measure that estimates the input activity of a MIMO system by only observing its outputs. This measure was introduced under the name *activity index*.

Activity index actually measures Mahalanobis distance [7]. Its implementation deploys second-order statistics. Related to MIMO models, it indicates the level of activity of individual input sources and is computed as follows:

$$p(n) = \mathbf{y}_e^T(n)\mathbf{R}_{\mathbf{y}_e}^{-1}\mathbf{y}_e(n) = \mathbf{t}_e^T(n)\mathbf{R}_{\mathbf{t}_e}^{-1}\mathbf{t}_e(n) \qquad (1)$$

where $\mathbf{R}_{\mathbf{t}_e}$ and $\mathbf{R}_{\mathbf{y}_e}$ stand for correlation matrices of model input source activity and model output observations,

respectively. Eq. (1) holds with exact equality in noise-free cases. In all cases, it depends on the extended system output observations $\mathbf{y}_e(n)$:

$$\mathbf{y}_e(n) = \mathbf{H}_e\mathbf{t}_e(n) + \mathbf{v}_e(n); n = 0,\ldots,N-1 \quad (2)$$

where subscript e designates extended vectors and matrices and N stands for the signal length. Extended output observations consist of:

$$\mathbf{y}_e(n) = [y_1(n),....,y_1(n- M_e+1),....,y_M(n),....,\\ y_M(n- M_e+1)]^T \quad (3)$$

where M_e stands for an extension factor.

Extended noise vector $\mathbf{v}_e(n)$ is considered constructed in the same way.

$\mathbf{H}_e$ contains the observed contributions of source symbols:

$$\mathbf{H}_e = \begin{bmatrix} \mathbf{H}_{11} & \cdots & \mathbf{H}_{1K} \\ \vdots & \ddots & \vdots \\ \mathbf{H}_{M1} & \cdots & \mathbf{H}_{MK} \end{bmatrix} \quad (4)$$

with M equals the number of observations, K the number of sources or source symbols, and

$$\mathbf{H}_{ij} = \begin{bmatrix} h_{ij}(0) & \cdots & h_{ij}(L-1) & 0 & \cdots & 0 \\ \vdots & \ddots & \vdots & \vdots & \ddots & \vdots \\ 0 & \cdots & h_{ij}(0) & h_{ij}(1) & \cdots & h_{ij}(L-1) \end{bmatrix} \quad (5)$$

where L means source symbol lengths. Vectors $\mathbf{t}_e(n)$ indicate instants of source firings at lag n:

$$\mathbf{t}_e(n) = [t_1(n),....,t_1(n- L- M_e+2),....,t_K(n),....,\\ t_K(n- L- M_e+2)]^T \quad (6)$$

where any element can be only either 0 or 1.

If the inequality

$$M \cdot M_e \geq K(L+M_e-1) \quad (7)$$

is fulfilled, the matrix $\mathbf{H}_e$ is of full column rank for K different observed symbols of length L and M observations.

The rest of the paper is based on the principles introduced and is organised as follows: Section II explains an extension of activity index to higher orders, Section III describes experimental results, while Section IV discusses the results and Section V concludes the paper.

II. Extension of Activity Index by Higher-Order Moments

Eq. (1) suggests the way the activity index is computed. By definition, correlation matrix of system output observations $\mathbf{y}_e$ yields:

$$\mathbf{R}_{\mathbf{y}_e} = \mathbf{y}_e\mathbf{y}_e^T = \mathbf{H}_e\mathbf{R}_{t_e}\mathbf{H}_e^T, \quad (8)$$

where ^{T} stands for matrix transpose. When the inverse of $\mathbf{R}_{\mathbf{y}_e}$ is pre- and post-multiplied by $\mathbf{y}_e$, convolution kernels $\mathbf{H}_e$ compensate:

$$\mathbf{y}_e^T(n)\mathbf{R}_{\mathbf{y}_e}^{-1}\mathbf{y}_e(n) = \mathbf{t}_e^T(n)\mathbf{H}^T\left(\mathbf{H}^T\right)^{-1}\mathbf{R}_{\mathbf{t}_e}^{-1}\mathbf{H}^{-1}\mathbf{H}\mathbf{t}_e(n) = \\ \mathbf{t}_e^T(n)\mathbf{R}_{\mathbf{t}_e}^{-1}\mathbf{t}_e(n) \quad (9)$$

and the right-hand side part of Eq. (1) becomes obvious. It is worth pointing out that activity index in its basic form, $p(n)$, is computed by second-order statistics, i.e. the correlation of observations, and that it depends exclusively on the input source contributions if the condition in (7) is verified. Experiments in [12] show that even when this condition is not fulfilled, i.e. in underdetermined cases, activity index represents a very robust measure of the response lengths and the number of the input sources.

A closer look at Eq. (9) reveals a very simple form of activity index when sources are strictly orthogonal, no noise is present, and condition (7) is fulfilled. Eq. (6) describes source firing pulse trains and shows that any source firing contributes to activity index $L+M_e$-1 non-zero samples of the same value. Such a sequence of samples always belongs to the same source. The samples' value depends on the diagonal elements related to that source in the inverse of correlation matrix of observations, $\mathbf{R}_{\mathbf{y}_e}^{-1}$. These elements equal the inverse of the number of firings that belong to the related source during the time of observation. Suppose a source activates 5 times during the system output measurement. Then, the diagonal elements in $\mathbf{R}_{\mathbf{y}_e}^{-1}$ for this source equal 1/5, and so does the corresponding activity index segment. A logical consequence of this fact is that the level of activity index depends on the source firing rate and the time of the system output observation. The higher the rate and the longer the time interval, the lower is the corresponding value of activity index.

In overdetermined cases without noise where source activities may overlap (sources are no longer orthogonal), values of activity index slightly change for all those positions that are influenced by system-response samples involved in superimpositions [12].

When the number of observations is too low to guarantee overdeterminancy and when noise is added to observations, the values of activity index samples become also dependent on the inferior convolution kernel compensation and noise energy. The lower signal-to-noise ratio (SNR) and the higher underdeterminancy, the weaker is the dependence of activity-index values on the number of firings of the observed source. Nevertheless, it has been observed that also in such situation activity index still alludes the overall level of source activity [12].

Experiments using non-linear extensions of signal observations in the CKC application have been reported in [13]. The problem of only one signal observation was tackled by the CKC decomposition. To increase the number of observations, every observed sample $y_i(n)$ was considered an independent random variable, and new, artificial observations were generated using higher-order moments of these variables. The same non-linear extension of observation was

also applied to the CKC decomposition of electrocardiograms [14].

Having all the previous work on the CKC and activity index in mind, we introduced a more general definition of activity index in [17]. We are recapitulating the derivation first and then confirming its importance by experiments. Dealing with the basic form, it is evident that the inverse of correlation matrix comprises inverses of the system channel responses $\mathbf{H}_e$–Eq. (9). In overdetermined cases with condition (7) verified, these responses are cancelled out when pre- and post-multiplied by $\mathbf{y}_e$. Keeping this fact in mind, similar schemes can be found if correlation is replaced by higher-order moments.

Redefine Eq. (3) as follows:

$$\mathbf{y}_e(n) = \Big[y_{e,1}(n),\ldots, y_{e,M_e}(n),\ldots, y_{e,(M-1)M_e+1}(n),\ldots, y_{e,MM_e}(n) \Big]^T \tag{10}$$

and treat $y_{e,i}(n)$; $i=1,\ldots,M\cdot M_e$ as random variables, as suggested in [13]. Thus, a matrix of the k-th order moments produced by these variables can be defined as

$$\mathbf{M}_k(\tau_1,\tau_2,\ldots,\tau_{k-1}) = E\left[\mathbf{y}_e(n)\otimes\mathbf{y}_e(n+\tau_1)\otimes\cdots\otimes\mathbf{y}_e(n+\tau_{k-1})\right] \tag{11}$$

where E stands for mathematical expectation, $\otimes$ for Kronecker product, and τ_1, τ_2, …, τ_{k-1} denote shifts of the extended observations $\mathbf{y}_e$ [16]. Matrix $\mathbf{M}_k$ is k-dimensional. Any 2D cross-section of this matrix can replace correlation matrix $\mathbf{R}_{\mathbf{y}_e}$ in the definition (1) of activity index.

Note that Eq. (1) requires the same observations that pre- and post-multiply the inverse of correlation matrix also involved in the correlation matrix computation. To fulfil this requirement, we have to divide the set of k repetitions of observations $\mathbf{y}_e$ from (11) into two subsets. Denote these two subsets by $\mathbf{Y}_{1,j}$ and $\mathbf{Y}_{j+1,k}$ and introduce the following definition:

$$\begin{aligned}\mathbf{Y}_{1,j}(n) &= \mathbf{y}_e(n)\circ\mathbf{y}_e(n+\tau_1)\circ\cdots\circ\mathbf{y}_e(n+\tau_{j-1})\\ \mathbf{Y}_{j+1,k}(n) &= \mathbf{y}_e(n+\tau_j)\circ\mathbf{y}_e(n+\tau_{j+1})\circ\cdots\circ \\ &\quad \mathbf{y}_e(n+\tau_{k-1})\end{aligned} \tag{12}$$

where the operator ○ stands for Hadamard (entrywise) product.

The generalised definition of activity index based on higher-order moments can now be written as:

$$p_k(n) = \mathbf{Y}_{1,j}^T(n)\mathbf{R}_{\mathbf{Y}}^{-1}\mathbf{Y}_{j+1,k}(n) \tag{13}$$

with

$$\mathbf{R}_{\mathbf{Y}} = \mathbf{Y}_{1,j}\mathbf{Y}_{j+1,k}^T .$$

As shown in [13] and [14], higher-moment extensions of observations proved beneficial when decomposing signals with few observations. On the other hand, activity index has also been used in the derivation of an important measure for the lengths of source responses. Higher-moment extensions of activity index, Eq. (13), are expected to open new insights into the signal mixture properties. Therefore, a comparison study on different activity index orders was conducted on synthetic signals. The basic goal of this study was to reveal what information this comparison can provide. The experiment and results are gathered in next sections.

III. Experiments with Synthetic Compound Signals

The most evident property of activity index is its dependence on the activity of sources. In noise-free cases this dependence mirrors only three source characteristics: their firing instants, the number of firings within entire observations, and the level of overlapping of source responses. When noise is taken into account, all three source properties still define the basic shape of activity index, but it can be smeared by the noise contributions considerably. Noise contributions cannot be easily estimated, because the noise in activity index means a projection of the observational noise from the space of observations to the space of sources. This transformation is caused by the inverse of system matrix $\mathbf{H}_e$, which is entirely unknown in real cases. However, the observational noise characteristics change when the observations are processed by higher moments, and so do the characteristics of the noise in different orders of activity index. Moreover, observation segments containing the superimpositions of source contributions are also modified differently because of the non-linear behaviour of higher-order moments. Putting all this together, it becomes evident that a comparison of different orders of activity index must single out the segments where simultaneous activity of sources appears and, vice versa, most probable segments with as few sources active as possible. This is what we were looking for in our experiments.

We experimented with the 3rd- and 4th-order activity indexes, $p_3(n)$ and $p_4(n)$, and compared them to the 2nd-order index, which actually is the basic activity index from Eq. (1). In all experimental runs, we adopted shifts $\tau_1 = \tau_2 = \ldots = \tau_{k-1} = 0$ (see Eq. (12)). This decision was taken mainly because the observations $\mathbf{y}_i$, $i = 1,\ldots, M$ are extended by factor M_e, Eq. (3), so that they are already shifted before entering higher-order moments. For the 3rd-order index we took into account $\mathbf{Y}_{1,1}$ and $\mathbf{Y}_{2,3}$ and for the 4th-order $\mathbf{Y}_{1,2}$ and $\mathbf{Y}_{3,4}$.

Our experiments involved synthetic signals of random source responses, $\mathbf{h}_{ij}$. The system inputs corresponded to sparse pulse trains in the following form:

$$t_j(n) = \sum_{l=-\infty}^{\infty}\delta(n-T_j(l)), \tag{14}$$

with unit-sample pulses placed at $T_j(l)$ lags. Minimum interpulse distance was kept longer than the length of source responses, L, thus eliminating any possibility of overlapping of two consecutive responses of the same source. T_j's were distributed according to Gaussian law, with a truncated negative tail due to the minimum interpulse distance. This limitation is characteristic in many practical situations, such

as in bioelectrical responses or transmitted symbols in communications.

As we have explained, the values of the activity index samples depend on the following factors: the number of source firings, i.e. the lengths of observations and source firing rates, the level of superimpositions, the fulfilment of condition (7), and SNR. The role of different lengths of observations is straightforward by being in a linear relationship with the index level, this is why we fixed the length of observations to only one value. We decided to influence the level of source superimpositions by three parameters: the number of sources, lengths of their responses, and their firing rates. We regulated the noise energy applying different SNRs. Finally, we also compared the cases with over- and underdeterminancy, which we managed by simulating different numbers of model output observations with different extensions.

A. Parameters and trials

Our experiments involved four different models that differ by the number of sources, K, their response lengths, L, number of observations, M, and number of observation extensions, M_e–see Eqs. (4) and (5):

- Model 1: $K = 5$, $L = 5$, $M = 10$, $M_e = 30$
- Model 2: $K = 5$, $L = 20$, $M = 10$, $M_e = 30$
- Model 3: $K = 20$, $L = 5$, $M = 50$, $M_e = 15$
- Model 4: $K = 20$, $L = 20$, $M = 50$, $M_e = 15$

All models were generated with random source responses whose samples were distributed according to uniform distribution, and all observations were of length $N = 2000$. In noise-free cases, activity index levels depend only on the number of source firings. This further depends on the source firing rate and the length of observations. Therefore we decided to generate the models form 1 to 4 in two different ways. In the first group of simulations we considered source firings identical for all the sources by fixing the mean interpulse distance at 200 samples with standard deviation of 20 samples–see Eq. (14). This caused any source to contribute to activity index by the same basic increment being equal to the inverse of source firing rates. Considering the lengths of observations and interpulse distances, the rate was 10, therefore the increments of activity indexes equal 0.1.

The second group of experiments examined the behaviour of activity indexes when sources fire with different rates. Such a situation is much more realistic, but it causes rather different increments related to different sources in activity indexes. The models for this group of simulations were based on randomly chosen interpulse distances between 70 and 300 samples and randomly chosen standard deviations between 7 and 30 samples. The two values were generated with even distribution over the sources. Once a pair was chosen for a source, it determined the firing conditions for this source throughout its activity.

Each model was involved in 30 Monte-Carlo simulation runs, and for every run 3 different noise conditions were considered: no noise, SNR of 20 dB, and SNR of 10 dB. Additive noise was random, zero-mean Gaussian in all cases.

For any model and source signals generated, activity indexes of orders 2, 3, and 4 were computed. Order 2 index was then subtracted from indexes of orders 3 and 4. These differences were statistically verified in order to find out possible regularities in behaviour of the three indexes.

It has been observed that any superimpositions of source activities generate phantom sources when higher-order indexes are computed [13]. Actually, the level of any higher-order activity index increases in the same way as if there were additional sources active in intervals where the activity of the original sources overlap. As this does not happen in the 2^{nd}-order index, a difference between a higher-order and the 2^{nd}-order index is supposed to be bigger in the intervals of superimpositions, as opposed to the intervals of fewer sources active.

To be able to assess the differences between indexes, we need a reference. It is rather straightforward to determine the intervals with superimpositions of source activity when dealing with simulations. If there is more than one pulse at any time position, n, in the extended sequences of source firings, $\mathbf{t}_e$ from Eq. (6), the number of simultaneous pulses indicates the number of overlapping sources. This measure was taken as a reference in all our experiments.

An example of activity indexes is given in Figs. 1 and 2, the former depicting the 3^{th}-order index (black dashed), 2^{nd}-order index (grey dotted), and the reference signal (grey solid), whereas the latter shows the same combination for the 4^{th}-order index.

IV. Simulation Results

Results of simulation for four models detailed in Subsection III.A are summarised in two groups of figures. First four figures show activity index differences for the simulations in which all the sources fire with the same frequency–Figs. 3 to 6. Next four figures correspond to the models whose sources fire with different, randomly chosen frequencies–Figs. 8 to 11. All the figures consist of two subplots: the upper one is related to the difference of activity index of the 3^{rd} and 2^{nd} order and the lower one is related to the difference of indexes of orders 4 and 2.

Activity indexes were computed at the 2^{nd}, 3^{rd}, and 4^{th} order with three levels of additive noise. Separate simulations were conducted for noise-free and noisy cases with SNRs of 20 dB and 10 dB. Indexes of length $N+M_e$ samples were segmented into several non-overlapping intervals according to the reference as described in the previous subsections. These intervals correspond to segments where different number of sources was active simultaneously, beginning with no sources active, and continuing with a single source active, any pair of sources active at the same time, any triplet of sources active at the same time, etc.

Parameters in Models 1 to 4 influence the behaviour of higher-order activity indexes also in dependence of the correlation matrix of observations being either over- or underdetermined. We wanted to investigate this dependence and set up the parameters to the values that caused the correlation matrices from Eqs. (1) and (13) overdetermined for the 2nd-order indexes in all the cases [10]. The correlation matrices for the 3rd- and 4th-order indexes were overdetermined only with Model 1, and underdetermined for other types of models.

Activity index differences in Figs. 3 to 6 are related to the experiments with sources that fired all at the same rate. These differences are averaged in intervals that were defined according to the number of overlapping sources, and qualified by their standard deviations (vertical bars) across 30 simulation runs.

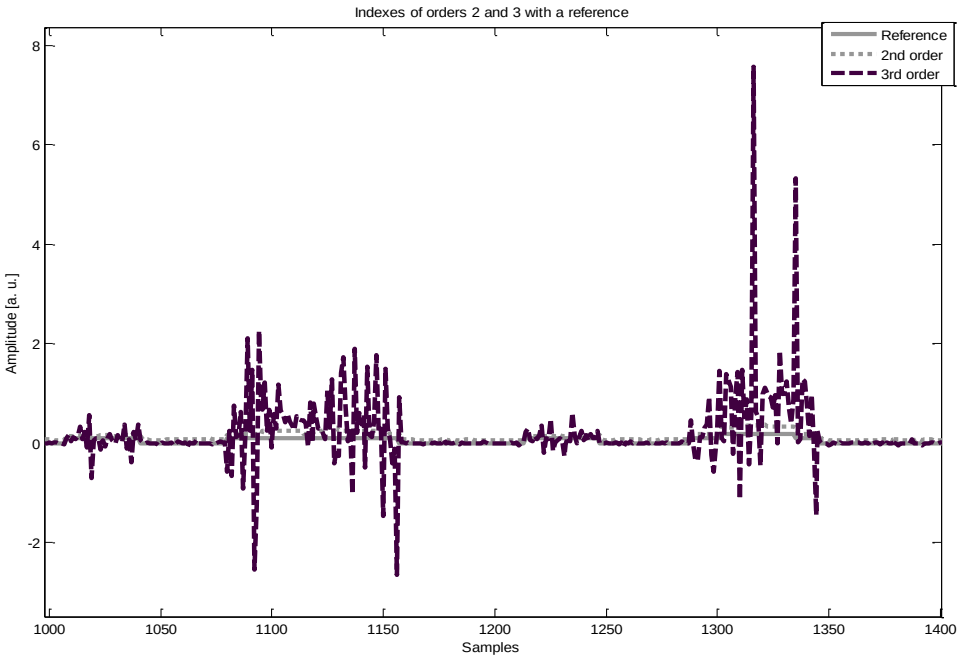

Figure 1: A segment of activity indexes in Model 1: 3rd order (black dashed), 2nd order (grey dotted), and reference (grey solid)

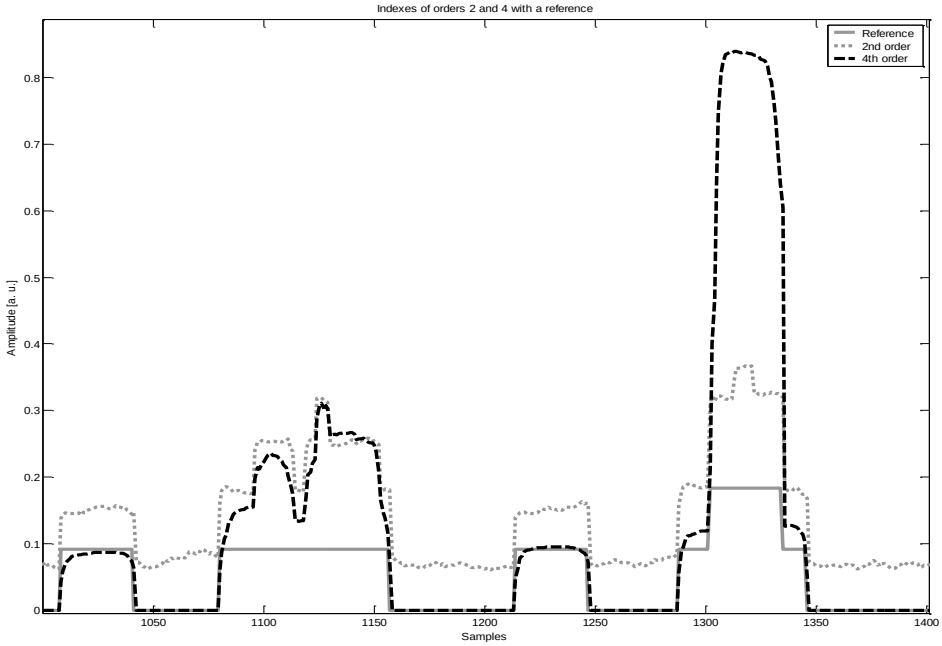

Figure 2: A segment of activity indexes in Model 1: 4th order (black dashed), 2nd order (grey dotted), and reference (grey solid)

Fig. 3 suggests that activity index, and the signal observations at the same time, can be segmented into the intervals with different number of active sources by a simple thresholding. Taking into account the standard deviations, it is evident that the 4th order varies significantly less than the 3rd order, even from 10 to 30 times less if 3 sources are active simultaneously and additive noise is present. Fig. 3 confirms this observation. An extreme case appeared with model 2 when the noise of 20 dB was added and the 3rd-order indexes were calculated. The mean 3rd- to 2nd-order difference rose even to 25 with standard deviation of 55 (this point falls far beyond the scale of Fig. 4, this is why it is not show in the figure). The reason for that is a high degree of noise in the 3rd-order activity index. A well know fact is that higher-order moments of odd orders suppress additive Gaussian noise [16]. For the calculation of activity index this means that the inverse of the correlation matrix loses its natural regularisation and, consequently, the observational noise is projected into the space of activity index with a much higher degree.

Fig. 7 illustrates the devastating effect of noise in indexes of the 3rd order. Only the influence of moderate additive noise with an SNR of 20 dB is depicted for Model 1. Indeed, the differences between the 3rd- and 2nd-order indexes clearly show high oscillations (grey dash-dotted), while the differences between the 4th- and 2nd-order indexes do not (black dashed). Differences in Fig. 7 are based on the indexes from Figs. 1 and 2, so that direct comparison of these figures is possible. Further investigations also proved that the 4th- to 2nd-order differences show rather low noise corruption, even when SNR equals 10 dB. And what is most beneficial, the 4th- to 2nd-order index differences follow the changes of the number of sources active in consecutive time intervals by a step-wise relationship, whose levels are rather stable and proportional to the number of simultaneously active sources. Therefore, signal segments with few sources active (ideally, only a single one) can be sorted out allowing for the different levels in the index differences. As a consequence, by initialising the compound signal decomposition, such as in [10], within signal segments with fewest active sources the more accurate and reliable decomposition results are guaranteed. It has to be mentioned, however, that the amplitudes of activity indexes decrease by increasing the number of sources and noise energy, which causes lower discriminancy and poorer signal segmentation.

Nevertheless, Figs. 4 to 6 prove that the 4th- to 2nd-order differences remain with the same amount of variance even when the number of overlapping sources increases for more than twice (from 3 in Fig. 3 to 8 in Fig. 6). Also the robustness of this measure remains constantly high as the influence of noise with SNRs down to 10 dB does not increase its variance noticeably.

On the other hand, differences of the 3rd- and 2nd-order activity indexes appear to be useless in a search of observation intervals with different levels of source overlapping. Their robustness is far too low. Fig. 7 clearly explains why it happens: the 3rd- to 2nd-order differences vary intensively throughout the observations, meaning that it is literally impossible to decide where signal segments with lower or higher level of source overlapping may begin or end.

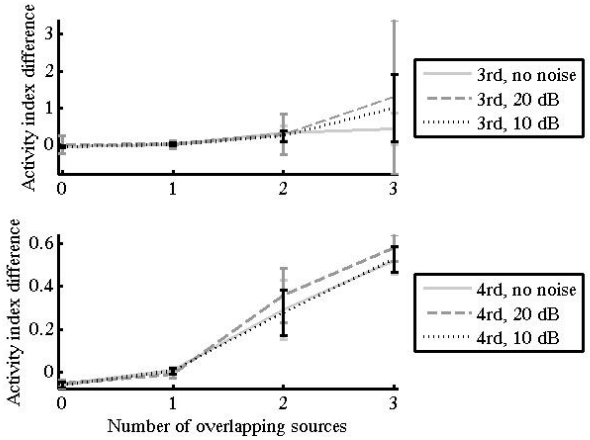

Figure 3: Model 1 with all sources at the same firing rate: differences of activity index means are depicted for the 3rd to 2nd order (upper graph) and the 4th to 2nd order (lower graph) versus the number of overlapping sources. Mean values and standard deviations were calculated in 30 Monte Carlo runs: light grey solid lines correspond to no noise in observations, grey dashed lines to SNRs of 20 dB, and black dotted lines to SNRs of 10 dB.

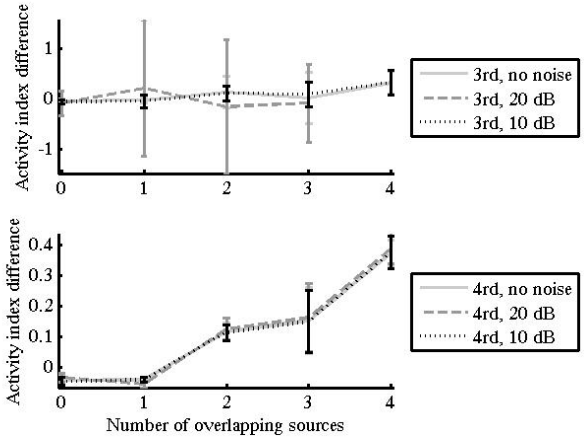

Figure 4: Model 2 with all sources at the same firing rate: differences of activity index means are depicted for the 3rd to 2nd order (upper graph) and the 4th to 2nd order (lower graph) versus the number of overlapping sources. Mean values and standard deviations were calculated in 30 Monte Carlo runs: light grey solid lines correspond to no noise in observations, grey dashed lines to SNRs of 20 dB, and black dotted lines to SNRs of 10 dB.

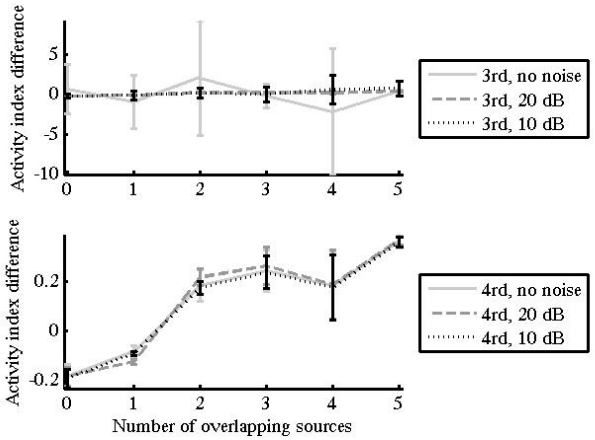

Figure 5: Model 3 with all sources at the same firing rate: differences of activity index means are depicted for the 3rd to 2nd order (upper graph) and the 4th to 2nd order (lower graph) versus the number of overlapping sources. Mean values and standard deviations were calculated in 30 Monte Carlo runs: light grey solid lines correspond to no noise in observations, grey dashed lines to SNRs of 20 dB, and black dotted lines to SNRs of 10 dB.

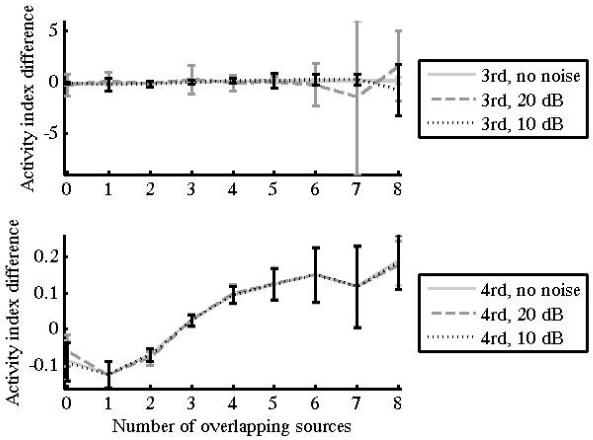

Figure 6: Model 4 with all sources at the same firing rate: differences of activity index means are depicted for the 3rd to 2nd order (upper graph) and the 4th to 2nd order (lower graph) versus the number of overlapping sources. Mean values and standard deviations were calculated in 30 Monte Carlo runs: light grey solid lines correspond to no noise in observations, grey dashed lines to SNRs of 20 dB, and black dotted lines to SNRs of 10 dB.

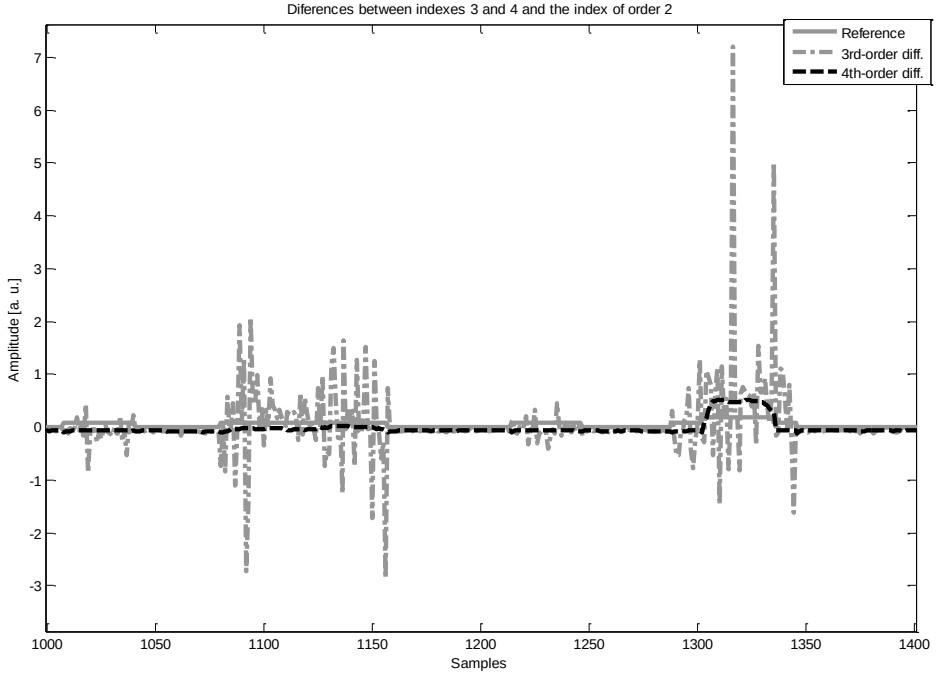

Figure 7: Differences of activity indexes in Model 1: 3rd to 2nd order (grey dash-dotted), 4th to 2nd order (black dashed), and reference (grey solid)

Inference on the effect of under- and overdeterminancy is also possible to some extent if we consider the fact that only Model 1 guarantees overdeterminancy entirely, while all other models tend to generate underdetermined activity index computations. Thus, Figs. 4 to 6 cover underdetermined cases and the only influence that can be attributed to the underdeterminancy is shown in a non-strict dependence of the activity index difference versus the number of simultaneously active sources (e.g. a drop with 7 overlapping sources in Fig. 6).

So far, the conclusions are based only on the first group of simulations with all sources having the same firing rate. A question arises whether a combination of sources firing at different rates may ruin the recognised advantages of the 4^{th}- to 2^{nd}-order activity index differences. The answer is given in Figs. 8 to 11. The 4^{th}- to 2^{nd}-order differences preserve all their beneficial properties and even the variability of the 3^{rd}- to 2^{nd}-order differences decreases, although not enough to judge this measure as acceptable. But the difference of the 4^{th}- to 2^{nd}-order activity indexes qualifies as a robust measure of source activity also in the cases when sources fire with different frequencies. This fact was not expected per se, because different firing rates mean also different levels of activity indexes. Nevertheless, the different contributions along activity indexes behave analogously in both the 2^{nd} and 4^{th} order. Their difference is therefore immune to different firing rates.

Our discussion confirms the 4^{th}- to 2^{nd}-order activity index differences can measure the source activity very robustly, because it is independent of the source properties, level of noise, and computational over- or underdeterminancy. Of course, it must be understood that this is not an absolute measure of the number of simultaneously active sources, but rather an indication of the level of overlapping of source activities observed in the outputs of MIMO systems.

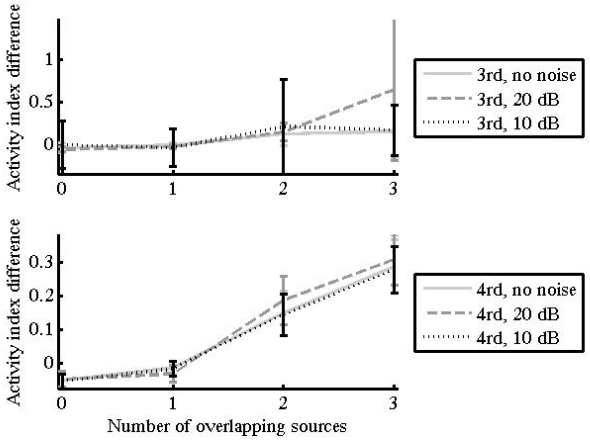

Figure 8: Model 1 with sources firing at different rates: differences of activity index means are depicted for the 3^{rd} to 2^{nd} order (upper graph) and the 4^{th} to 2^{nd} order (lower graph) versus the number of overlapping sources. Mean values and standard deviations were calculated in 30 Monte Carlo runs: light grey solid lines correspond to no noise in observations, grey dashed lines to SNRs of 20 dB, and black dotted lines to SNRs of 10 dB.

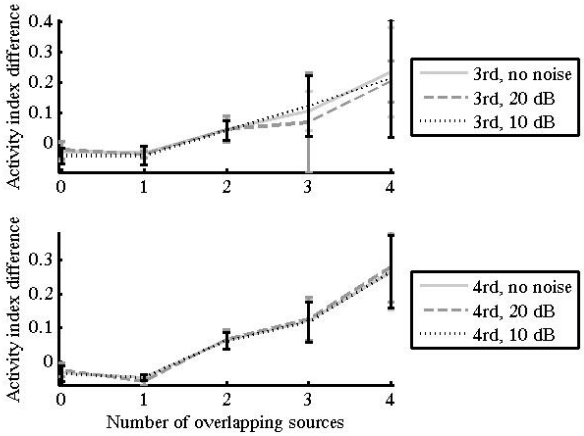

Figure 9: Model 2 with sources firing at different rates: differences of activity index means are depicted for the 3^{rd} to 2^{nd} order (upper graph) and the 4^{th} to 2^{nd} order (lower graph) versus the number of overlapping sources. Mean values and standard deviations were calculated in 30 Monte Carlo runs: light grey solid lines correspond to no noise in observations, grey dashed lines to SNRs of 20 dB, and black dotted lines to SNRs of 10 dB.

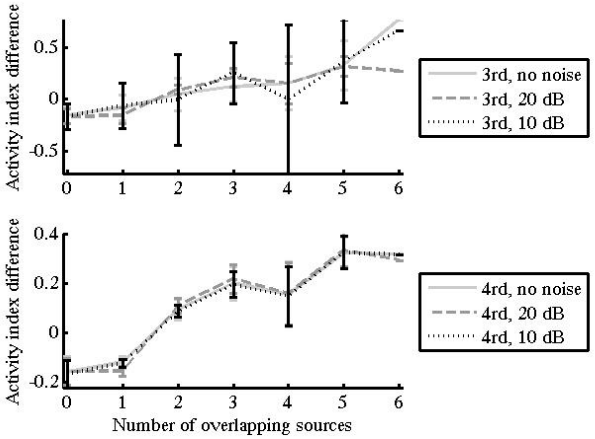

Figure 10: Model 3 with sources firing at different rates: differences of activity index means are depicted for the 3^{rd} to 2^{nd} order (upper graph) and the 4^{th} to 2^{nd} order (lower graph) versus the number of overlapping sources. Mean values and standard deviations were calculated in 30 Monte Carlo runs: light grey solid lines correspond to no noise in observations, grey dashed lines to SNRs of 20 dB, and black dotted lines to SNRs of 10 dB.

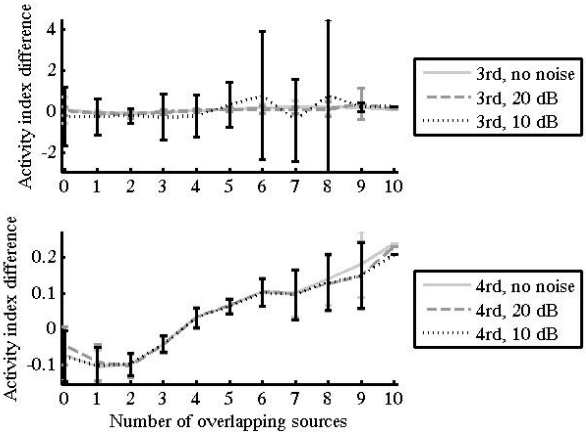

Figure 11: Model 4 with sources firing at different rates: differences of activity index means are depicted for the 3^{rd} to 2^{nd} order (upper graph) and the 4^{th} to 2^{nd} order (lower graph) versus the number of overlapping sources. Mean values and standard deviations were calculated in 30 Monte Carlo runs: light grey solid lines correspond to no noise in observations, grey dashed lines to SNRs of 20 dB, and black dotted lines to SNRs of 10 dB.

V. Conclusion

The proposed definition of activity indexes based on higher-order moments leads to interesting conclusions. The most important one proves the difference between the 4^{th}- and 2^{nd}-order activity index can point out the observation signal segments with a different number of active sources. The difference is proportionally higher where the number of simultaneously active sources is higher. Even more important fact is that the corresponding levels of the difference function are stable and noise-resistant, which makes them a suitable measure when looking for the signal segments with minimum overlapping of source activity. This information is beneficial if avoiding higher levels of source superimpositions is necessary. A practical example is the initialisation of the CKC decomposition: when it is done within signal segments with as few sources active as possible, the decomposition results may be expected optimum.

Acknowledgment

This work was in part supported by the Slovenian Research Programme Funding Scheme P2-0041.

References

[1] U. Madhow, "Blind Adaptive interference suppression for direct-sequence CDMA," *Proceedings of the IEEE*, vol. 86, no. 10, 1998, pp. 2049-2069.

[2] G. Desodt, D. Muller, "Complex independent components analysis applied to the separation of radar signals," in *Signal Processing V, Theories and applications*, pp. 665-668, 1994.

[3] R. Gribonval, "Sparse decomposition of stereo signals with matching pursuit and application to blind separation of more than two sources from a stereo mixture," in *Proceedings of ICASSP'02,* 2002, pp. III-3057–III-3060.

[4] A. K. Barros, A. Mansour, N. Ohnishi, "Removing artefacts from ECG signals using independent components analysis," *Neurocomputing*, vol. 22, 1999, pp. 173-186.

[5] A. Hyvärinen, M. Inki, "Estimating overcomplete independent component bases for image windows," *Journal of Mathematical Imaging and Vision*, vol. 17, 2002, pp. 139-152.

[6] Bin. Gao, W. L. Woo and S. S. Dlay, "Single Channel Audio Source Separation," *WSEAS Transactions on Signal Processing*, April 2008, vol. 4, iss. 4, pp. 173-182.

[7] A. de Medeiros Martins, A. Duarte Dória Neto, J. Dantas de Melo, "Comparison Between Mahalanobis Distance and Kullback-Leibler Divergence in Clustering Analysis," *WSEAS Transactions on Systems*, April 2004, vol. 3, iss. 2, pp. 501-506.

[8] A. Holobar, D. Zazula, "Correlation-based approach to separation of surface electromyograms at low contraction forces," *Med. & Biol. Eng. & Comput*., vol. 42, no. 4, 2004, pp. 487-496.

[9] C. J. De Luca, P. J. Foley, Z. Erim, "Motor unit control properties in constant-force isometric contractions," *J. of Neurophysiol*., vol. 76, no. 3, 1996, pp. 1503-1516.

[10] A. Holobar, D. Zazula, "Multichannel blind source separation using convolution kernel compensation," *IEEE trans. signal process.*, vol. 55, iss. 9, Sept. 2007, pp. 4487-4496.

[11] V. Glaser, A. Holobar, D. Zazula, "Decomposition of synthetic surface electromyograms using sequential convolution kernel compensation," *WSEAS Trans. Biol. Biomed*., Jul. 2008, vol. 5, iss. 7, pp. 143-152.

[12] R. Istenič, D. Zazula, "Activity index as an indicator of the number of signal sources," *WSEAS trans. signal process.*, vol. 4, iss. 9, Sept. 2008, pp. 542-551.

[13] D. Zazula, A. Holobar, "Blind source separation based on a single observation," in *Proceedings of the 2nd international workshop on biosignal processing and classification, BPC 2006, in conjunction with ICINCO 2006*, Setúbal, Portugal, August 2006, pp. 76-85.

[14] D. Zazula, A. Holobar, F. Angely, "Analysis of electrocardiograms using the convolution kernel compensation approach," in *Proceedings of 2007 14th International Workshop on Systems, Signals and Image Processing (IWSSIP) and 6th EURASIP Conference Focused on Speech & Image Processing, Multimedia Communications and Services (EC-SPIMCS)*, 2007, pp. 1-4.

[15] R. Istenič, A. Holobar, M. Gazzoni, D. Zazula, "Motor control information extracted from surface EMG as muscle force estimation," *WSEAS Trans. Biol. Biomed.*, Jan. 2008, vol. 5, iss. 1, pp. 1-11.

[16] C.L. Nikias, A.P. Petropulu, Higher-Order Spectra Analysis, Prentice-Hall, Englewood Cliffs, NJ, 1993.

[17] D. Zazula, R. Istenič, "Properties of activity index extended by higher-order moments," in *Proceedings of the 4th International Conference on Circuits, Systems and Signal (CSS'10)*, Corfu Island, Greece, July 22-25, 2010, pp. 151-157.